A Theoretical Investigation of the Reactions of N(^{2}D) with Small Alkynes and Implications for the Prebiotic Chemistry of Titan

Luca Mancini[1(✉)], Emília Valença Ferreira de Aragão[1,3], Marzio Rosi[2], Dimitrios Skouteris[3], and Nadia Balucani[1]

[1] Dipartimento di Chimica, Biologia e Biotecnologie, Università degli Studi di Perugia, 06123 Perugia, Italy
{luca.mancini2, emilia.dearagao}@studenti.unipg.it, nadia.balucani@unipg.it
[2] Dipartimento di Ingegneria Civile e Ambientale, Università degli Studi di Perugia, 06125 Perugia, Italy
marzio.rosi@unipg.it
[3] Master-Up, Via Sicilia 41, 06128 Perugia, Italy
d.skouteris@master-up.it

Abstract. The reactions between atomic nitrogen, in its first electronically excited state (^{2}D), and two different hydrocarbons, methyl acetylene and acetylene, have been analyzed by performing electronic structure calculations of the potential energy surface. For each reaction, H-displacement channels leading to cyclic molecular products have been identified, together with an H_2 elimination channel for the reaction N(^{2}D) + acetylene and a methyl (CH_3) loss channel for the N(^{2}D) + methylacetylene reaction. Since both reactions have been found to be exothermic and without an entrance barrier, we suggest that they are fast and efficient under the conditions of the upper atmosphere of Titan. These data will be used to perform kinetic calculations and will be compared with detailed experimental results in future work.

Keywords: Ab initio calculations · Titan atmosphere · Astrochemistry

1 Introduction

The chemistry of nitrogen atoms in their first electronically excited state ^{2}D is of great relevance in several extraterrestrial environments, such as the upper atmosphere of Titan (the largest moon of Saturn) and Pluto [1–5]. One of the few moons of the Solar System which possess thick atmospheres, Titan has attracted the attention of the scientific community because of possible similarities with primitive Earth [3]. Due to the fact that the appearance of life on Earth has drastically modified our planet, it is impossible to reconstruct the first steps in the evolution of prebiotic chemistry and, thus, the study of planets or moons which share similarities with primitive Earth has become fundamental for its understanding [3–5]. Interesting data about Titan became available starting from the Voyager missions, which reported molecular nitrogen (N_2) as the major component of its atmosphere [6], with minor constituents being methane

© Springer Nature Switzerland AG 2020
O. Gervasi et al. (Eds.): ICCSA 2020, LNCS 12251, pp. 717–729, 2020.
https://doi.org/10.1007/978-3-030-58808-3_52

and higher hydrocarbons (e.g. ethane, ethylene, acetylene, etc.) [7]. Methylacetylene was also observed [8] while the presence of its structural isomer allene, predicted to be present by photochemical models, was confirmed only very recently [9].

Our understanding of the chemistry of the atmosphere of Titan relies on a multidisciplinary approach. First of all, observation, performed with the support of both space mission and ground-based instruments, allows one to derive the abundances of trace compounds which are indicators of an active atmospheric chemistry. As a complement, laboratory experiments aiming at reproducing the conditions of Titan can furnish a first look into the dominant chemical processes (see, for instance, Refs. [10–12] and references therein). Finally, a more refined approach is based on photochemical models that include physical and chemical parameters (see, for instance, Refs. [13–16]), with the latter being determined in theoretical and/or experimental investigations. To build a photochemical model able to reproduce the abundance of the chemical species present in trace amounts (which are also those with a strong prebiotic potential) it is imperative to know the reaction rates of all relevant elementary reactions [16].

Since the first photochemical model developed by Yung et al. [13] after the Voyager mission, one of the starting steps that initiate the chemistry of nitrogen is considered to be the dissociation of molecular nitrogen in the thermosphere induced by free electrons:

$$N_2 + e^- \rightarrow N(^4S) + N(^2D) + e^- \quad (1)$$

The dissociation of molecular nitrogen leads to the formation of atomic nitrogen in the ground, ^4S, and first electronically excited, $^2D_{5/2,3/2}$, states. The ^2D state is metastable with a long radiative lifetime of *ca* 48 h [1], has an energy content of 230.0 kJ/mol with respect to the ground state and is produced in a large amount also by the EUV photodissociation of N_2 as well as by the electron recombination of the N_2^+ ions [1]. Nitrogen atoms can then react with the hydrocarbons present in the upper atmosphere leading to the formation of N-containing organic compounds, some of which were detected at the time of the Voyager 1 mission [7, 8]. Remarkably, while atomic nitrogen in the ground state is not a very reactive species (only its reactions with open-shell radicals are fast enough to be of any relevance in the conditions of the upper atmosphere of Titan), the reactions of $N(^2D)$ have been invoked to explain the formation of molecules containing a novel C-N bond [13]. Numerous reactions involving $N(^2D)$ and the most common hydrocarbons in the atmosphere of Titan, as well as molecular hydrogen and water, have been already investigated from both an experimental and a theoretical point of view (namely, $N(^2D) + C_2H_2$, C_2H_4, C_2H_6, C_6H_6 [17–26]). More specifically, on the side of theoretical calculations, a combined approach has been used in which the overall potential energy surface has been determined via electronic structure calculations at the DFT and CCSD(T) levels of theory. The resulting stationary points along the minimum energy path have been used to perform kinetic calculations, using a Rice-Ramsperger-Kassel-Marcus (RRKM) code implemented for this purpose [17]. The comparison with the experimental data, coming from the crossed molecular beams (CMB) experiments, allows the derivation of the reaction mechanism.

In this preliminary account, we report on dedicated electronic structure calculations of the stationary points of the potential energy surfaces (PESs) for the reactions involving the two simplest alkynes, that is, ethyne (or acetylene) and propyne (or methylacetylene):

$$N(^2D) + C_2H_2 \rightarrow HCCN + H \quad (2a)$$

$$\rightarrow H_2 + C_2N \quad (2b)$$

$$N(^2D) + CH_3CCH \rightarrow H + C_3H_3N \quad (3a)$$

$$\rightarrow CH_3 + C_2NH \quad (3b)$$

Previous theoretical investigations at a different level of theory are available for the reaction (2) [18, 27, 28], while, to the best of our knowledge, no data are available for reaction (3). The present results will be used to perform kinetic calculations to obtain rate coefficients and product branching ratios to be compared with the experimental results obtained in the CMB experiments with mass spectrometric detection in a future work.

2 Computational Details

The $[C_2H_2 + N]$ and $[C_3H_4 + N]$ reactions have been analyzed by exclusively considering the lowest doublet electronic state for both systems. The PESs for the two systems have been characterized through optimization of the most stable stationary points, adopting a computational strategy which has already been utilized successfully in several cases [17, 20, 26, 29–35]. In particular, density functional calculations have been performed at the B3LYP [36, 37] level of theory in conjunction with the correlation consistent valence polarized basis set aug-cc-pVTZ [38–40]. The harmonic vibrational frequencies have been computed at the same level of theory in order to determine the nature of each stationary point, i.e. minimum if all the frequencies are real and saddle point if there is one, and only one, imaginary frequency. Intrinsic reaction coordinates (IRC) calculations [41, 42] have been performed in order to assign the saddle points. Then, the energy of each stationary point has been computed with the more accurate coupled cluster theory including both single and double excitations and using a perturbative estimate of the effect of the triple excitations (the CCSD(T) level) [43–45], with the same basis set aug-cc-pVTZ. The zero-point correction (computed using the scaled harmonic vibrational frequencies obtained at the B3LYP/aug-cc-pVTZ level) has been added in order to correct the energies at 0 K. The experimental [46] separation N(^{4}S) − N(^{2}D) of 230.0 kJ/mol has been added to the energy of N(^{4}S) at all the levels of calculations in order to estimate the energy of N(^{2}D). All calculations have been carried out using GAUSSIAN 09 [47] while the analysis of the vibrational frequencies has been done using MOLDEN [48, 49].

3 Results

3.1 N(^{2}D) + Acetylene

In the PES for the system N(^{2}D) + acetylene, shown below in Fig. 1, three cyclic minima have been located (MIN1AC, MIN2AC, MIN3AC), connected by three transition states (TS1AC, connecting MIN1AC and MIN2AC, TS2AC, connecting MIN1AC and MIN3AC, and TS3AC, connecting MIN2AC and MIN3AC). The same stationary points were previously investigated by Takayanagi et al. in 1998 at the MP2/cc-pVTZ level for geometry optimization and MP4(full, SDTQ)/cc-pVTZ level for the energy evaluation [27]. We can notice a reasonable agreement between the calculations, considering the different levels of theory, except for the presence of a barrier of 2.9 kcal/mol at the MP4(full, SDTQ)/cc-pVTZ level, which has not been identified at the CCSD(T) level. We investigated the initial attack of N(^{2}D) also at the B2PLYP/aug-cc-pVTZ level of theory in order to include the second order perturbation theory in the calculations. Neither method allows us to locate the barrier. In Fig. 2 a comparison of the geometries of the reactant and the first intermediate optimized at B3LYP/aug-cc-pVTZ and B2PLYP/aug-cc-pVTZ level of theory is shown.

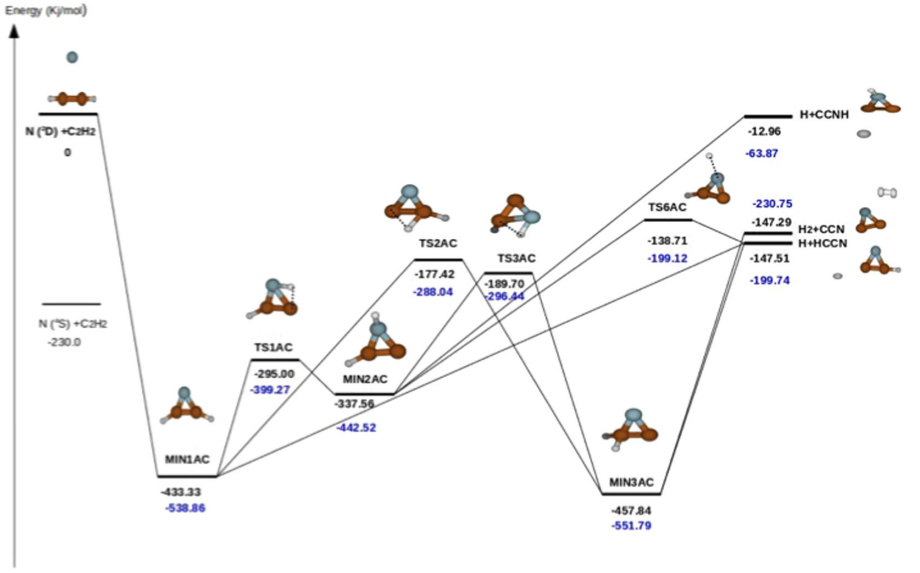


Fig. 1. Schematic representation of the PES obtained for the system N(^{2}D) + acetylene, with the relative energies (kJ/mol) evaluated at the CCSD(T)/aug-cc-pVTZ (in black) and B3LYP/aug-cc-pVTZ (in blue) levels of theory. (Colour figure online)

The absence of an entrance barrier was also verified by very accurate calculations by Nuñez-Reyes *et al.* [28], that accompanied an experimental determination of the reaction rate coefficient. Notably, the value of the rate coefficient derived by the kinetic experiments carried out by Nuñez-Reyes *et al.* [28] is very large and, together with the temperature dependence, points to a barrierless reaction.

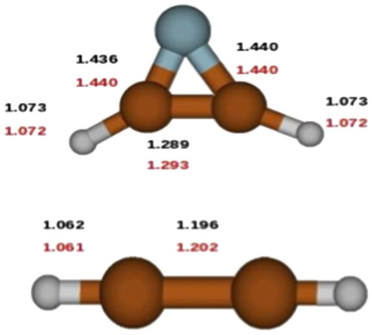


Fig. 2. Geometries of the reactant and the first intermediate (distances in angstroms) optimized at B3LYP/aug-cc-pVTZ (in black) and B2PLYP/aug-cc-pVTZ levels of theory (in red). (Color figure online)

In summary, we can conclude that the reaction starts with the barrierless addition of N(^{2}D) to the triple bond of acetylene. The addition leads to the formation of a cyclic intermediate MIN1AC, in which two C-N bonds are present. The MIN1AC intermediate can then isomerize to MIN2AC by overcoming the transition state TS1AC, which is characterized by the shift of an H atom from one of the C atoms to the N atom, with the consequent formation of a new N-H bond. Finally, two different sequences can lead to the formation of the third intermediate MIN3AC, which is the most stable species in the C_2NH_2 PES: *a)* the isomerization of MIN1AC through the transition state TS2AC (overcoming a barrier of 243.63 kJ/mol), and *b)* the isomerization of MIN2AC through the transition state TS3AC (overcoming a barrier of 147.86 kJ/mol).

In addition to the isomerization processes, all the three intermediates can lead to the formation of different products by losing an H atom. In particular, MIN1AC can directly decompose into H and the cyclic fragment HCCN (which shows a relative energy, with respect to the reactant asymptote, of −147.51 kJ/mol). MIN2AC can lose an H atom and form either the cyclic C(NH)C radical (−12.96 kJ/mol with respect to the reactant asymptote) and cyclic HC(N)C (−147.51 kJ/mol with respect to the reactant asymptote), through a transition state (TS6AC, −138.71 kJ/mol) which clearly shows the breaking of the N-H bond. Finally, MIN3AC can also form both C(NH)C and HC(N)C by losing an H atom or the cyclic fragment CCN by an H_2-elimination mechanism (this channel is located at −147.29 kJ/mol with respect to the reactant asymptote). All identified stationary points lie under the reactant energy asymptote.

The structures of the minima and transition states optimized at the B3LYP/aug-cc-pVTZ level of theory are shown in Fig. 3. Table 1 reports on the enthalpy changes and barrier heights for each step, computed at the CCSD(T)/aug-cc-pVTZ level of theory.

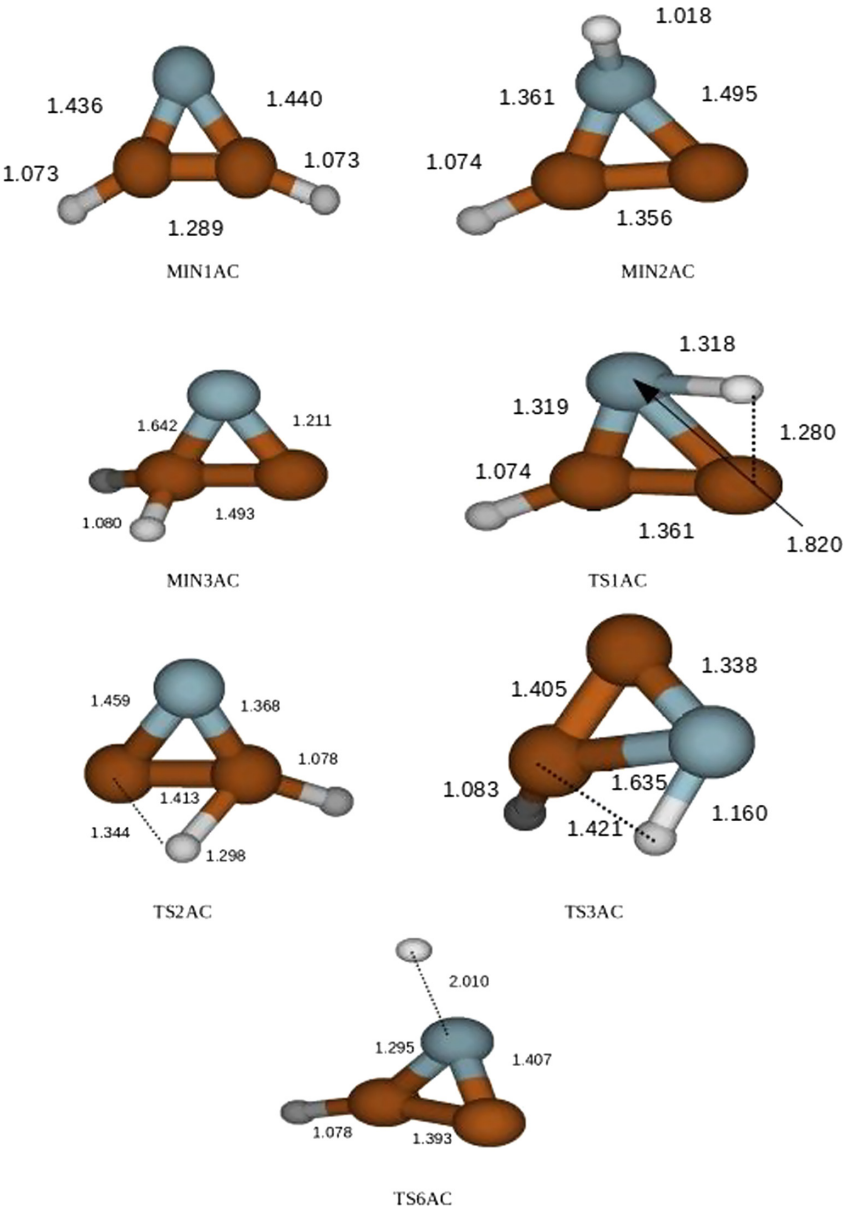


Fig. 3. Optimized structures calculated at the B3LYP/aug-cc-pVTZ level of theory of the minima and transition states for the N(^{2}D) + acetylene reaction (distances in angstroms).

Table 1. Enthalpy changes (kJ/mol) and barrier heights (kJ/mol) computed at the CCSD(T)/aug-cc-pVTZ level of theory for the reaction of the system N(^{2}D) + acetylene.

	ΔH_0^0	Barrier heights
N(^{2}D)+C_2H_2 → MIN1AC	−433.33	
MIN1AC → H+HCCN	285.82	
MIN1AC → MIN2AC	95.77	138.33
MIN1AC → MIN3AC	−24.51	255.91
MIN2AC → H+CCNH	324.6	
MIN2AC → H+HCCN	190.05	198.85
MIN2AC → MIN3AC	−120.28	147.86
MIN3AC → H+HCCN	310.33	
MIN3AC → H_2+CCN	310.55	

3.2 N(^{2}D) + Methylacetylene

Figure 4 shows the schematic PES for the reaction N(^{2}D) + methylacetylene, in which three cyclic minima can be identified (MIN1MA, MIN2MA and MIN3MA), linked by two transition states (TS1MA, connecting MIN1MA and MIN2MA, and TS4MA, connecting MIN2MA and MIN3MA). As in the previous system, the reaction starts with a barrierless addition of N(^{2}D) to the triple bond of the methylacetylene molecule, leading to the formation of the cyclic intermediate MIN1MA (located at −446.15 kJ/mol with respect to the reactant energy asymptote). This structure can generate different products depending on which bond undergoes fission. Two different barrierless channels can lead to the loss of atomic hydrogen, one leading to the isomer $H_3CC(N)C$ (the resulting exothermicity of this channel is −166.18 kJ/mol) by the fission of the acetylenic CH bond, and one leading to the isomer $H_2CC(N)CH$ (the resulting exothermicity of this channel is −220.15 kJ/mol) by the fission of one of the CH bonds of the methyl group. Moreover, the intermediate MIN1MA can undergo a C-C bond breaking with the formation of CH_3 + cyclic-C(N)CH. MIN2MA can be easily formed via isomerization of MIN1MA overcoming a barrier of 140.6 kJ/mol. The related transition state clearly exhibits the breaking of a C-H bond in the methyl group and simultaneous formation of a N-H bond. The new intermediate can, in turn, dissociate forming atomic hydrogen and the cyclic molecule $H_2CC(NH)C$ (the resulting exothermicity of this channel is −90.17 kJ/mol) or the isomer $H_3CC(N)C$, also formed by the dissociation of MIN1MA. MIN2MA can also undergo an isomerization process to produce the third intermediate MIN3MA, which is the lowest minimum along the PES. MIN3MA can undergo a decomposition with the formation of atomic hydrogen and $H_3CC(N)C$ or CH_3 and C(N)CH. All identified stationary points lie under the reactant energy asymptote. In Fig. 5 the optimized structure of the minima and transition states identified in the potential energy surface at the B3LYP/aug-cc-pVTZ level of theory are reported, while in Table 2 the enthalpy changes and barrier heights for each step of the reaction are shown.

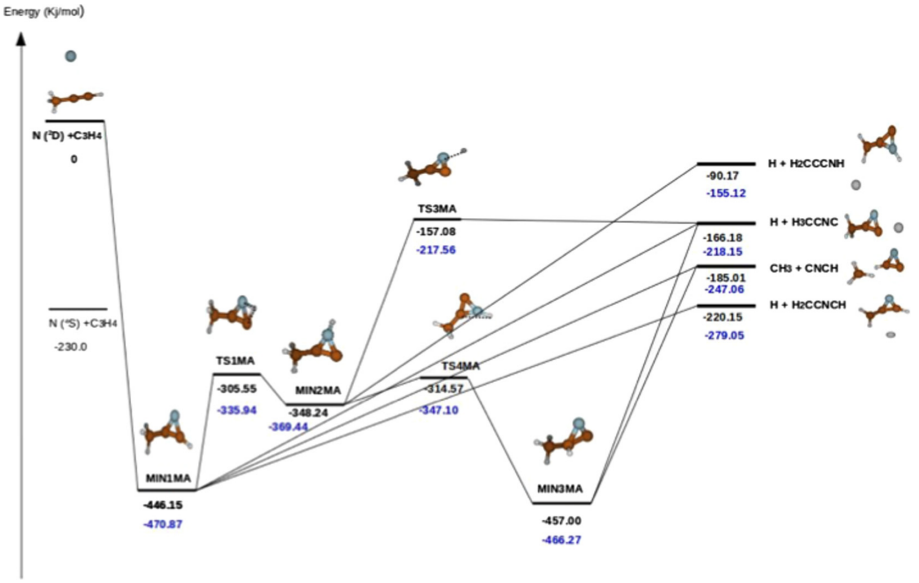


Fig. 4. Schematic representation of the PES obtained for the N(^{2}D) + methylacetylene reaction, with the relative energies (kJ/mol) evaluated at the CCSD(T)/aug-cc-pVTZ (in black) and B3LYP/aug-cc-pVTZ (in blue) levels of theory. (Color figure online)

4 Discussion

As expected, the two reactions N(^{2}D) + C_2H_2 and N(^{2}D) + CH_3CCH share several similarities as far as their initial steps are concerned. The electrophilic nature of N(^{2}D) drives its attack toward the electron density of the triple bond present in both C_2H_2 and CH_3CCH molecules. As a result, a first cyclic intermediate is formed in both cases, where the nitrogen atom is bound to the two acetylenic carbon atoms. When the co-reactant is methylacetylene, the presence of a -CH_3 group makes the addition intermediate asymmetric and more channels become open because of the possibility of losing a CH_3 moiety. It is also possible to lose an H atom from the methyl group with the formation of the cyclic product $H_2CC(NH)C$. As a consequence, the reaction with methylacetylene is much more complex than the reaction with acetylene, as already observed in many other cases (for instance, see the reactions of atomic oxygen, CN radicals or BO radicals with acetylene as opposed to methylacetylene [50–54]).

From previous investigations on the reaction N(^{2}D) + C_2H_2 [18] we know that additional reaction pathways are possible following the ring-opening of the MIN2AC cyclic intermediate with the formation of (almost) linear HCCN and/or HNCC + H. These pathways and their analogues for the N(^{2}D) + CH_3CCH system have not been investigated in the present study, but will be characterized in a future work.

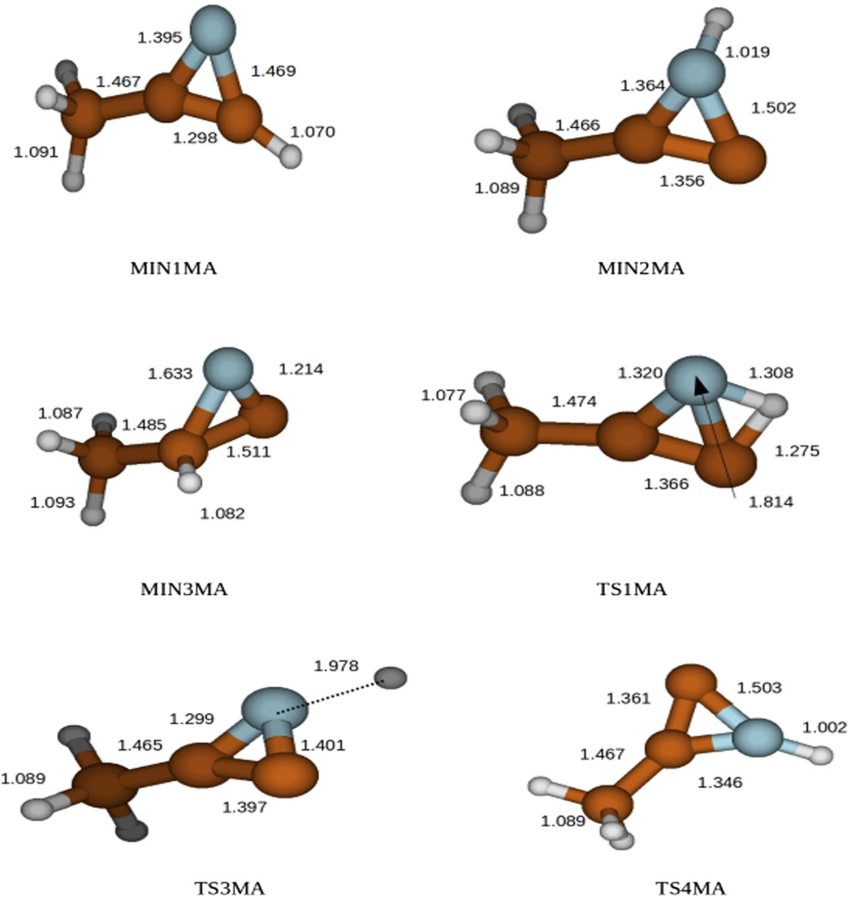


Fig. 5. Optimized structures calculated at the B3LYP/aug-cc-pVTZ level of theory of the minima and transition states for the N(^{2}D)+methyl acetylene reaction (distances in angstroms).

Table 2. Enthalpy changes (kJ/mol) and barrier heights (kJ/mol) computed at the CCSD(T)/aug-cc-pVTZ level of theory for the reaction of the system N(^{2}D) + methylacetylene.

	ΔH_0^0	Barrier heights
C_3H_4 → MIN1MA	−446.15	
MIN1MA → H+H_2CCNCH	226.00	
MIN1MA → CH_3+CNCH	261.14	
MIN1MA→ H+H_3CCNC	279.97	
MIN1MA→ MIN2MA	97.91	140.6
MIN2MA → H+H_2CCCNH	258.07	
MIN2MA → H+H_3CCNC	182.06	191.16
MIN2MA → MIN3MA	−108.76	33.67
MIN3MA → CH_3+CNCH	271.99	
MIN3MA → H+H_3CCNC	290.82	

5 Conclusions

In the present work, electronic structure calculations have been employed in order to derive the potential energy surface for two reactions of relevance in different natural environments, such as terrestrial and planetary atmospheres. The $N(^2D)$ addition processes have been found to be barrierless for the analyzed systems at all the employed levels of theory. Furthermore, the identified stationary points for the two processes lie below the reactant energy asymptote, therefore the global reactions are feasible under the low temperature conditions of Titan. Kinetic calculations are required to derive the rate constants and branching ratios of the two processes. The derived kinetic parameters will allow us to include the title reactions in the chemical models of the atmosphere of Titan and of other bodies of the Solar System where the molecules involved are present. The present study can be combined with the results coming from experimental investigations, such as CMB experiments, in order to understand the overall reaction mechanism.

Acknowledgments. This research was supported by the Italian Space Agency (ASI, DC-VUM-2017-034, Grant no 2019-3 U.O Life in Space).

References

1. Dutuit, O., et al.: Critical review of N, N^+, N_2^+, N^{++} and N_2^{++} main production processes and reactions of relevance to Titan's atmosphere. Astrophys. J. Suppl. Ser. **204**, 20 (2013)
2. Vuitton, V., Dutuit, O., Smith, M.A., Balucani, N.: Chemistry of Titan's atmosphere. In: Mueller-Wodarg, I., Griffith, C., Lellouch, E., Cravens, T. (eds.) Titan: Surface, Atmosphere and Magnetosphere. Cambridge University Press, Cambridge (2013)
3. Balucani, N.: Nitrogen fixation by photochemistry in the atmosphere of titan and implications for prebiotic chemistry. In: Trigo-Rodriguez, J., Raulin, F., Muller, C., Nixon, C. (eds.) The Early Evolution of the Atmospheres of Terrestrial Planets. Astrophysics and Space Science Proceedings, vol. 35, pp. 155–164. Springer, New York (2013). https://doi.org/10.1007/978-1-4614-5191-4_12
4. Balucani, N.: Elementary reactions of N atoms with hydrocarbons: first steps towards the formation of prebiotic N-containing molecules in planetary atmospheres. Chem. Soc. Rev. **41**, 5473–5483 (2012)
5. Balucani, N.: Elementary reactions and their role in gas-phase prebiotic chemistry. Int. J. Mol. Sci. **10**, 2304–2335 (2009)
6. Lindal, G.F., Wood, G.E., Hotz, H.B., Sweetnam, D.N. Eshleman, V.R., Tyler, G.L.: The atmosphere of Titan. An analysis of the Voyager 1 radio occultation measurements. Icarus **2** (53), 348–363 (1983)
7. Hanel, R., et al.: Infrared Observations of the Saturnian System from Voyager 1. Science **212** (4491), 192–200 (1981)
8. Maguire, W.C., Hanel, R.A., Jennings, D.E., Kunde, V.G., Samuelson, R.E.: C_3H_8 and C_3H_4 in Titan's atmosphere. Nature **292**(5825), 683–686 (1981)
9. Lombardo, N.A., et al.: Detection of propadiene on Titan. Astrophys. J. Lett. **881**, L33 (2019). (6 pp)
10. Imanaka, H., Smith, M.A.: Formation of nitrogenated organic aerosols in the Titan upper atmosphere. PNAS **107**, 12423–12428 (2010)

11. Somogyi, A., Oh, C.H., Smith, M.A., Lunine, J.I.: Organic environments on Saturn's moon, Titan: simulating chemical reactions and analyzing products by FT-ICR and ion-trap mass spectrometry. J. Am. Soc. Mass Spectrom. **16**(6), 850–859 (2005)
12. Cassidy, T., et al.: Radiolysis and photolysis of icy satellite surface: experiments and theory. Space Sci. Rev. **153**, 299–315 (2010)
13. Yung, K.L., Allen, M., Pinto, J.P.: Photochemistry of the atmosphere of Titan: comparison between models and observations. Astrophys. J. Suppl. Ser. **55**, 465–506 (1984)
14. Lavvas, P., Coustenis, A., Vardavas, I.: Coupling photochemistry with haze formation in Titan's atmosphere, Part I: model description. Planet. Space Sci. **56**, 27 (2008)
15. Lavvas, P., Coustenis, A., Vardavas, I.: Coupling photochemistry with haze formation in Titan's atmosphere, Part II: results and validation with Cassini/Huygens data. Planet. Space Sci. **56**, 67 (2008)
16. Hébrard, E., Dobrijevic, M., Bénilan, Y., Raulin, F.: Photochemical kinetics uncertainties in modeling Titan's atmosphere: first consequences. Planet. Space Sci. **55**, 1470–1489 (2007)
17. Balucani, N., Bergeat, A., Cartechini, L., Volpi, G.G., Casavecchia, P., Skouteris, D., Rosi, M.: Combined crossed molecular beam and theoretical studies of the N(^{2}D) + CH_4 reaction and implications for atmospheric models of Titan. J. Phys. Chem. A **113**, 11138–11152 (2009)
18. Balucani, N., et al.: Cyanomethylene formation from the reaction of excited nitrogen atoms with acetylene: a crossed beam and ab initio study. J. Am. Chem. Soc. **122**, 4443–4450 (2000)
19. Balucani, N., Leonori, F., Petrucci, R., Stazi, M., Skouteris, D., Rosi, M., Casavecchia, P.: Formation of nitriles and imines in the atmosphere of Titan: combined crossed-beam and theoretical studies on the reaction dynamics of excited nitrogen atoms N(^{2}D) with ethane. Faraday Discuss. **147**, 189–216 (2010)
20. Balucani, N., et al.: Combined crossed beam and theoretical studies of the N(^{2}D) + C_2H_4 reaction and implications for atmospheric models of Titan. J. Phys. Chem. A **116**, 10467–10479 (2012)
21. Balucani, N., Cartechini, L., Alagia, M., Casavecchia, P., Volpi, G.G.: Observation of nitrogen-bearing organic molecules from reactions of nitrogen atoms with hydrocarbons: a crossed beam study of N(^{2}D) + ethylene. J. Phys. Chem. A **104**, 5655–5659 (2000)
22. Balucani, N., et al.: Dynamics of the N(^{2}D) + D_2 reaction from crossed-beam and quasiclassical trajectory studies. J. Phys. Chem. A **105**, 2414–2422 (2001)
23. Balucani, N., et al.: Experimental and theoretical differential cross sections for the N(^{2}D)+H_2 reaction. J. Phys. Chem. A **110**, 817–829 (2006)
24. Homayoon, Z., Bowman, J.M., Balucani, N., Casavecchia, P.: Quasiclassical trajectory calculations of the N(^{2}D) + H_2O reaction elucidating the formation mechanism of HNO and HON seen in molecular beam experiments. J. Phys. Chem. Lett. **5**, 3508–3513 (2014)
25. Balucani, N., Cartechini, L., Casavecchia, P., Homayoon, Z., Bowman, J.M.: A combined crossed molecular beam and quasiclassical trajectory study of the Titan-relevant N(^{2}D) + D_2O reaction. Mol. Phys. **113**, 2296–2301 (2015)
26. Balucani, N., Pacifici, L., Skouteris, D., Caracciolo, A., Casavecchia, P., Rosi, M.: A theoretical investigation of the reaction N(^{2}D) + C_6H_6 and implications for the upper atmosphere of Titan. In: Gervasi, O., et al. (eds.) ICCSA 2018. LNCS, vol. 10961, pp. 763–772. Springer, Cham (2018). https://doi.org/10.1007/978-3-319-95165-2_53
27. Takayanagi, T., et al.: Measurements of thermal rate constants and theoretical calculations for the N(^{2}D, ^{2}P) + C_2H_2 and C_2D_2 reactions. J. Phys. Chem. A **102**, 6251–6258 (1998)
28. Nuñez-Reyes, D., Loison, J.-C., Hickson, K.M., Dobrijevic, M.: Rate constants for the N(^{2}D) + C_2H_2 reaction over the 50–296 k temperature range. Phys. Chem. Chem. Phys. **21**, 22230–22237 (2019)

29. Falcinelli, S., Rosi, M., Cavalli, S., Pirani, F., Vecchiocattivi, F.: Stereoselectivity in autoionization reactions of hydrogenated molecules by metastable gas atoms: the role of electronic couplings. Chem. Eur. J. **22**, 12518–12526 (2016)
30. Leonori, F., et al.: Crossed-beam and theoretical studies of the $S(^1D) + C_2H_2$ reaction. J. Phys. Chem. A **113**, 4330–4339 (2009)
31. Bartolomei, M., Cappelletti, D., De Petris, G., Moix Teixidor, M., Pirani, F., Rosi, M., Vecchiocattivi, F.: The intermolecular potential in NO-N_2 and $(NO\text{-}N_2)^+$ systems: implications for the neutralization of ionic molecular aggregates. Phys. Chem. Chem. Phys. **10**, 5993–6001 (2008)
32. De Petris, G., Cartoni, A., Rosi, M., Barone, V., Puzzarini, C., Troiani, A.: The proton affinity and gas-phase basicity of sulfur dioxide. ChemPhysChem **12**, 112–115 (2011)
33. Leonori, F., et al.: Observation of organosulfur products (thiovinoxy, thioketene and thioformyl) in crossed-beam experiments and low temperature rate coefficients for the reaction $S(^1D) + C_2H_4$. Phys. Chem. Chem. Phys. **11**, 4701–4706 (2009)
34. De Petris, G., Rosi, M., Troiani, A.: SSOH and HSSO radicals: an experimental and theoretical study of $[S_2OH]^{0/+/-}$ species. J. Phys. Chem. A **111**, 6526–6533 (2007)
35. Rosi, M., Falcinelli, S., Balucani, N., Casavecchia, P., Leonori, F., Skouteris, D.: Theoretical study of reactions relevant for atmospheric models of titan: interaction of excited nitrogen atoms with small hydrocarbons. In: Murgante, B., et al. (eds.) ICCSA 2012. LNCS, vol. 7333, pp. 331–344. Springer, Heidelberg (2012). https://doi.org/10.1007/978-3-642-31125-3_26
36. Becke, A.D.: A new mixing of Hartree-Fock and local density-functional theories. J. Chem. Phys. **98**(2), 1372–1377 (1998)
37. Stephens, P.J., Devlin, F.J., Chablowski, C.F., Frisch, M.J.: Ab initio calculation of vibrational absorption and circular dichroism spectra using density functional force fields. J. Phys. Chem. **98**(45), 11623–11627 (1994)
38. Dunning, T.H., Jr.: Gaussian basis sets for use in correlated molecular calculations. I. The atoms boron through neon and hydrogen. J. Chem. Phys. **90**, 1007–1023 (1989)
39. Woon, D.E., Dunning, T.H., Jr.: Gaussian basis sets for use in correlated molecular calculations. III. The atoms aluminum through argon. J. Chem. Phys. **98**, 1358–1371 (1993)
40. Kendall, R.A., Dunning Jr., T.H., Harrison, J.R.: Electron affinities of the first-row atoms revisited. Systematic basis sets and wave functions. J. Chem. Phys. **96**, 6796–6806 (1992)
41. Gonzalez, C., Schlegel, H.B.: An improved algorithm for reaction path following. J. Chem. Phys. **90**, 2154–2161 (1989)
42. Gonzalez, C., Schlegel, H.B.: Reaction path following in mass-weighted internal coordinates. J. Phys. Chem. **94**, 5523–5527 (1990)
43. Bartlett, R.J.: Many-body perturbation theory and coupled cluster theory for electron correlation in molecules. Annu. Rev. Phys. Chem. **32**, 359–401 (1981)
44. Raghavachari, K., Trucks, G.W., Pople, J.A., Head-Gordon, M.: Quadratic configuration interaction. A general technique for determining electron correlation energies. Chem. Phys. Lett. **157**, 479–483 (1989)
45. Olsen, J., Jorgensen, P., Koch, H., Balkova, A., Bartlett, R.J.: Full configuration–interaction and state of the art correlation calculations on water in a valence double-zeta basis with polarization functions. J. Chem. Phys. **104**, 8007–8015 (1996)
46. Schofield, K.: Critically evaluated rate constants for gaseous reactions of several electronically excited species. J. Phys. Chem. Ref. Data **8**, 723–798 (1979)
47. Frisch, M.J., et al.: Gaussian 09, Revision A.02. Gaussian, Inc., Wallingford CT (2009)
48. Schaftenaar, G., Noordik, J.H.: Molden: a pre- and post-processing program for molecular and electronic structures. J. Comput. Aided Mol. Des. **14**, 123–134 (2000)

49. Schaftenaar, G., Vlieg, E., Vriend, G.: Molden 2.0: quantum chemistry meets proteins. J. Comput. Aided Mol. Des. **31**(9), 789–800 (2017). https://doi.org/10.1007/s10822-017-0042-5
50. Leonori, F., Balucani, N., Capozza, G., Segoloni, E., Volpi, G.G., Casavecchia, P.: Dynamics of the O(^{3}P) + C_2H_2 reaction from crossed molecular beam experiments with soft electron ionization detection. Phys. Chem. Chem. Physiscs **16**, 10008–10022 (2014)
51. Gimondi, I., Cavallotti, C., Vanuzzo, G., Balucani, N., Casavecchia, P.: Reaction dynamics of O(^{3}P) + Propyne: II. Primary products, branching ratios, and role of intersystem crossing from ab initio coupled triplet/singlet potential energy surfaces and statistical calculations. J. Physycal Chem. A **120**(27), 4619–4633 (2016)
52. Kaiser, R.I., Balucani, N.: Exploring the gas phase synthesis of the elusive class of boronyls and the mechanism of boronyl radical reactions under single collision conditions. Acc. Chem. Res. **50**, 1154–1162 (2017)
53. Huang, L.C.L., et al.: Crossed beam reaction of the cyano radical with hydrocarbons molecule. IV. Chemical dynamics of cyanoacetylene (HCCCN; $X^1\Sigma^+$) formation from reaction of CN($X^2\Sigma^+$) with acetylene, C_2H_2 ($X^1\Sigma_g^+$). J. Chem. Phys. **113**, 8656 (2000)
54. Balucani, N., Asvany, O., Kaiser, R.I., Osamura, Y.: Formation of three C4H3N isomers from the reaction of CN ($X^2\Sigma^+$) with Allene, H2CCCH2 (X^1A^1), and methylacetylene, CH3CCH (X^1A^1): a combined crossed beam and ab initio study. J. Phys. Chem. A **106**, 4301–4311 (2002)